

Fron.Chem. Res, 2026, Vol: 3, Issue: 2, pages: 37-43.

Frontiers in Chemical Research

Research article

Ilam University

Molecular Dynamics Simulation of Poly (acrylic acid) as a Liner at Rubber–Rubber Interfaces in the Presence of Nitrate Ester Plasticizers

Dariush Fallah*

*Faculty of Chemistry and Chemical Engineering, Malek Ashtar University of Technology, Tehran, Iran

Received: 12 Oct 2026
Accepted: 06 Nov 2026
Published online: 07 Nov 2026

Abstract In this study, poly(acrylic acid) (PAA) was investigated as a novel liner material with the potential to absorb polar plasticizers. Molecular dynamics simulations of PAA in combination with TEGDN, BTTN, and TMETN plasticizers were conducted for 500 ps under controlled temperature and pressure using the Nose thermostat and Berendsen barostat. The binding energy, radial distribution functions (RDFs), solubility parameters, and mechanical propertiesof the simulated systems were evaluated to assess intermolecular interactions, compatibility, and the potential performance of PAA as a plasticizer-absorbing liner. The calculated binding energies for TEGDN, BTTN, and TMETN plasticizers were 82.79, 40.02, and 50.51 kcal.mol-1, respectively, suggesting favorable interactions between these plasticizers and poly(acrylic acid) (PAA). Furthermore, the solubility parameter results suggested favorable miscibility between PAA and all three plasticizers. The calculated Young's moduli of PAA in the presence of TEGDN, BTTN, and TMETN were 8.92, 11.62, and 5.96 GPa, respectively, indicating differences in the mechanical responses of the simulated systems. The intermolecular radial distribution function (RDF) profiles revealed structural correlations between PAA and the plasticizer molecules. Although these features provide insights into the local molecular arrangements, they do not independently establish the nature of the underlying interactions or provide direct evidence of miscibility. Nevertheless, the binding-energy results and solubility parameter differences suggest favorable interactions and potential compatibility between PAA and the investigated plasticizers.

Keywords: Molecular Dynamics Simulation, polyacrylic acid, Nitrate Ester Plasticizer, Compatibility, Liner

1.Introduction

Bonding two polymer layers made of different materials is often required for various applications [1]. These layers may gradually separate from each other over several years, causing the multilayer system to lose its functionality. Various factors, including mechanical stresses, thermal stresses, transportation-related stresses, and stresses encountered during operation, can contribute to interfacial debonding between the polymer layers [2,3]. Identifying the underlying causes of such failures at rubber – rubber interfaces can provide valuable insights into preventing interfacial debonding [4]. One of the most important chemical factors contributing to interfacial separation and crack formation is the difference in polarity between the plasticizers and the polymers [5] (Figure 1). Plasticizers used in these layers are often polar, whereas the polymers, such as polybutadiene, are nonpolar [6]. This polarity mismatch can promote plasticizer migration over time, leading to its accumulation at the interface between the layers [6]. Such migration can ultimately weaken interfacial adhesion and cause debonding between the two rubber layers. One approach to addressing this problem is the use of liners. Liners are thin polymeric layers placed between two rubber surfaces that, after curing, form an elastomeric interlayer between them [7]. Conventional liners primarily serve to promote adhesion between the two layers [7]. However, next-generation liners are designed with plasticizer-absorbing capabilities, allowing plasticizers migrating from the rubber layers to diffuse into the liner rather than accumulate at the interface between the two rubber layers [8]. This approach can help preserve interfacial adhesion and reduce the risk of debonding. The design and development of a novel liner require extensive experimental testing. One of the most effective approaches to reducing development costs is the use of simulation techniques to predict liner properties before experimental fabrication. Various computational methods based on molecular dynamics and quantum mechanics have been developed for this purpose. However, polymers typically require computationally intensive calculations due to their large molecular structures. Molecular dynamics is one of the most effective methods for predicting the properties of polymers and evaluating their interactions with different plasticizers [9-11]. Molecular dynamics simulations can provide valuable predictions of plasticizer absorption by a liner by evaluating the compatibility between the polymer and the plasticizer. The compatibility of various polymers with polar plasticizers has been extensively investigated using molecular dynamics simulations. These studies have examined systems involving Polyvinyl Chloride (PVC) [12], inert polymers and plasticizers [13], biopolymers [14], fluoropolymers, ammonium dinitramide [15], and other related materials. The results have provided useful frameworks for predicting polymer–plasticizer compatibility and understanding the intermolecular interactions governing these systems. Poly(acrylic acid) (PAA) is a polar polymer with a strong potential to absorb polar plasticizers. It can be synthesized through free-radical polymerization, a relatively simple and straightforward polymerization technique. Considering its physical and structural properties, poly(acrylic acid) (PAA) is expected to have potential for application as a liner material [16]. In the proposed application, the PAA-based liner is intended to function as an absorption-based anti-migration layer between two rubber components. Its purpose is not to prevent the plasticizer from migrating out of the first rubber component, but rather to capture the plasticizer released from this component and limit its subsequent penetration into the second rubber component. In this configuration, the liner acts as an intermediate layer that absorbs and retains the migrated plasticizer, thereby reducing its potential transfer to the adjacent rubber material. Accordingly, the ability of PAA to interact with and accommodate nitrate ester plasticizers is an important consideration in evaluating its potential suitability for this application. The present study therefore focuses on investigating the molecular-level interactions and compatibility of PAA with selected nitrate ester plasticizers as a preliminary step toward assessing its potential use as an anti-

doi: 10.22034/fcr.2026.2108660.1034

Corresponding author: Dariush Fallah, Email: Fallah.dariush@mut.ac.ir

migration liner. In this study, a novel liner was designed and evaluated using molecular dynamics simulations based on NPT ensemble calculations (Figure 2). Poly(acrylic acid) (PAA) was investigated as a specialized liner material, and its miscibility with three polar plasticizers (TEGDN, BTTN, or TMETN) was assessed. Key parameters influencing compatibility, including binding energy, radial distribution functions, solubility parameters, and mechanical properties, were evaluated to investigate the intermolecular interactions and the potential suitability of PAA as a liner material.

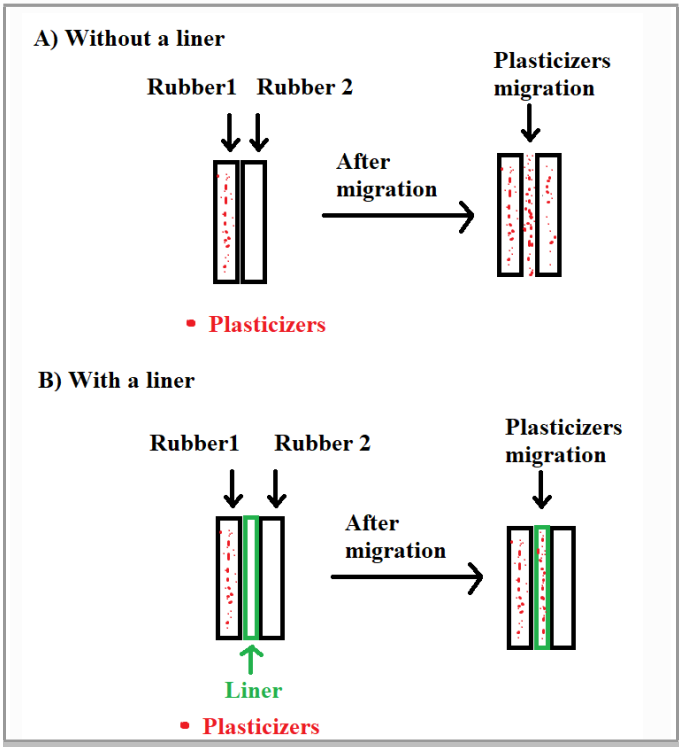


Figure 1. Plasticizer migration at the interface between two rubber layers in the presence and absence of a liner.

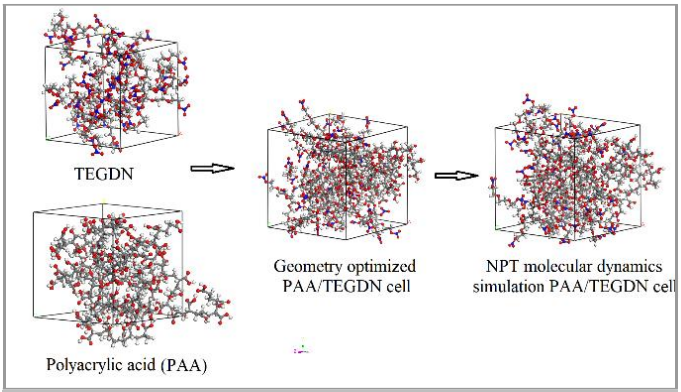


Fig 2. Simulated Compatibility Pattern of Polyacrylic Acid and TEGDN.

2.Simulation Methodology

2.1. Simulation

Molecular dynamics calculations were performed using Materials Studio 2023.

2.2. Methodology

Molecular dynamics simulations were performed using Materials Studio to investigate bulk mixtures of poly(acrylic acid) (PAA) with three nitrate ester plasticizers (BTTN, TMETN, and TEGDN). Molecular structures were optimized using the COMPASS III force field in the Forcite module. Each amorphous-cell model contained five PAA chains, each comprising 20 repeat units, together with 30 molecules of one plasticizer (TEGDN, BTTN, or TMETN). Because the plasticizer molecular weights differ, the use of the same number of plasticizer molecules does not by itself establish an identical 50:50 mass composition across the three systems; accordingly, the composition is specified here by the modeled molecule counts rather than asserting an unverified equal mass fraction. The cells were optimized and then subjected to NPT molecular dynamics simulations at 298 K and 1 atm for 500 ps. The Nose thermostat and Berendsen barostat were used to control temperature and pressure, respectively. Other simulation settings (including integration timestep, electrostatic treatment, van der Waals cutoff, charge assignment, coupling constants, and trajectory sampling interval) are not specified in the source manuscript and must be checked against the original Forcite project before they can be reported. The simulation settings reported in this study are limited to the parameters documented in the available simulation records. Additional Forcite parameters, including the integration time step, electrostatic treatment, van der Waals cutoff, charge assignment method, coupling constants, and trajectory-sampling interval, could not be independently verified and are therefore not specified

3.Results and discussion

To investigate poly(acrylic acid) (PAA) as a novel liner material, its molecular interactions and compatibility with rubber surfaces must be evaluated. The absorption of plasticizers migrating from the rubber matrix remains a significant challenge, and one commonly employed approach involves the use of absorbent liners. These liners often exhibit suitable mechanical properties, helping maintain interfacial integrity and prevent debonding between the liner and the rubber. The molecular structures of PAA and the TEGDN, BTTN, and TMETN plasticizers were initially energy-minimized using the Smart algorithm, as shown in Figure 3. Amorphous cells were then constructed using the molecule counts described above and optimized using the Smart algorithm with a maximum of 5000 iterations (Figure 4). The present model is a finite-chain, uncrosslinked bulk mixture. It does not reproduce a crosslinked or entangled liner network, nor does it include either rubber phase. Consequently, the calculations characterize the modeled PAA–plasticizer mixtures and cannot directly establish compatibility with rubber surfaces or interfacial performance. In practical liner applications, the absorption of approximately 10 wt% plasticizer may be sufficient to provide satisfactory liner performance. Nevertheless, a higher plasticizer loading of 50 wt% was considered in the present study as an upper-limit condition to investigate the maximum potential plasticizer-uptake capacity of PAA. Each simulation system was designed as a binary PAA–plasticizer mixture, with the intention of considering a 50/50 wt% composition, consisting of 50 wt% PAA and 50 wt% of one selected nitrate ester plasticizer (TEGDN, BTTN, or TMETN). Each plasticizer was investigated separately. The selected high-loading condition was intended to provide insight into the molecular interactions and potential absorption capacity of PAA under relatively demanding conditions. It should be noted that the actual weight fractions of the constructed simulation cells depend on the molecular masses and numbers of molecules used; therefore, the exact composition of each model cell is reported separately.

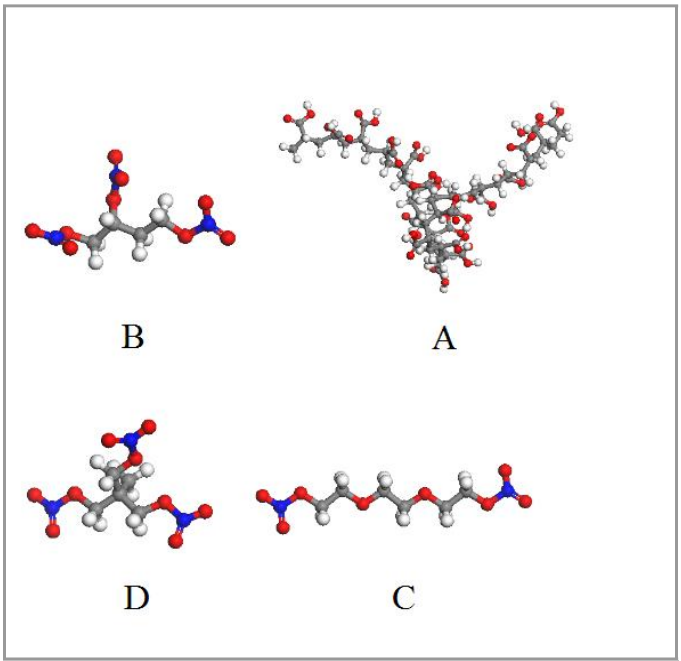


Fig 3. Optimized structures of (a) polyacrylic acid, (b) BTTN, (c) TEGDN, and (d) TMETN.

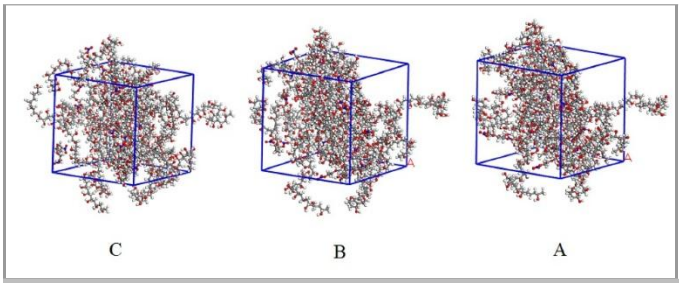


Fig 4. Simulated pathway: (a) as-prepared amorphous cell, (b) energy-minimized cell, and (c) cell after molecular dynamics simulation (PAA/TEGDN).

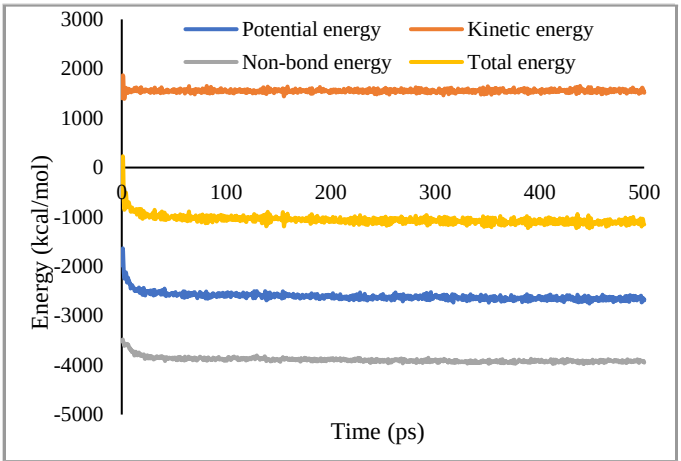


Fig 5. Time evolution of the kinetic, potential, non-bonded, and total energies during the 500 ps molecular dynamics simulation (PAA/TEGDN).

Figure 5 presents the kinetic, potential, non-bonded, and total energies monitored during the 500 ps molecular dynamics simulations. The simulations were conducted at a target temperature of 298 K and pressure of 1 atm using the Nose thermostat and Berendsen barostat. Changes in monitored energy components can be used to assess relaxation during the trajectory; however, the duration of 500 ps and apparent stabilization of selected quantities alone do not prove complete configurational equilibration. No independent simulation replicas or statistical uncertainty estimates are reported in the source data; conclusions that require such evidence are therefore treated cautiously.

Figures 6–9 show the temperature, density, cell angles, and cell lengths recorded during the simulations. These monitored quantities provide information about the evolution of the simulation cells over 500 ps. Although their trajectories may indicate relaxation or apparent stabilization, the available information does not establish rigorous configurational convergence or reproducibility across independent replicas.

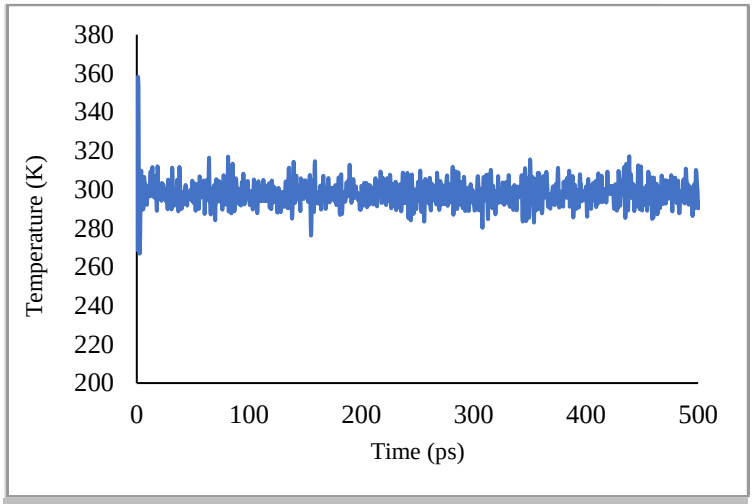


Fig 6. Temperature profile during the 500 ps molecular dynamics simulation (PAA/TEGDN)

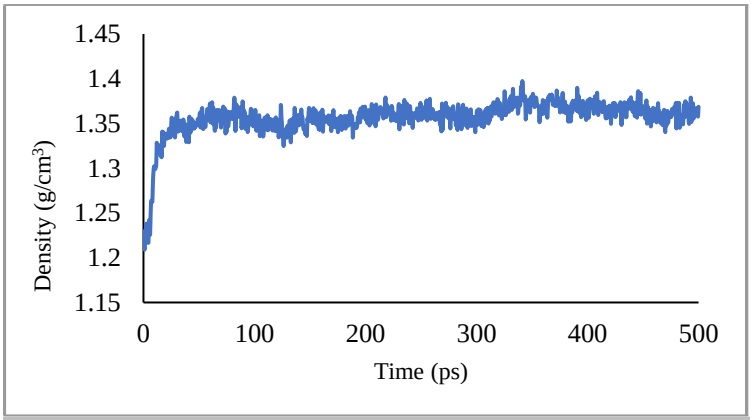


Fig 7. Density profile during the 500 ps molecular dynamics simulation (PAA/TEGDN).

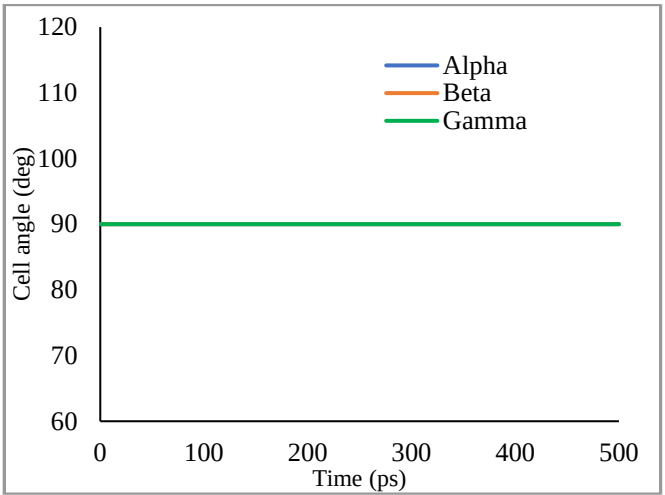


Fig 8. Cell-angle evolution during the 500 ps molecular dynamics simulation (PAA/TEGDN).

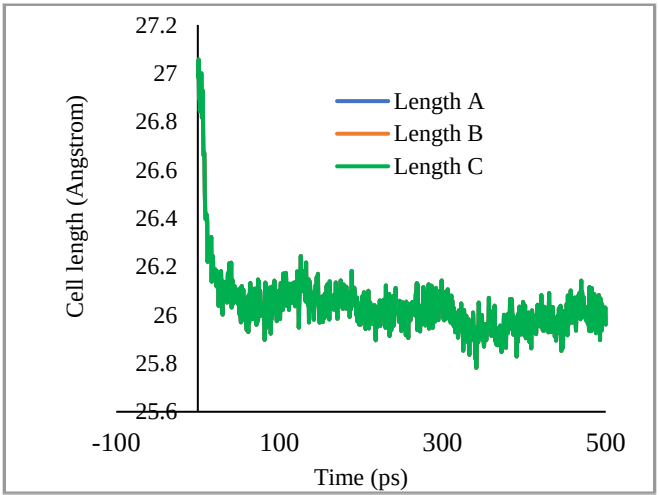


Fig 9. Cell-length evolution during the 500 ps molecular dynamics simulation (PAA/TEGDN).

3.1. Binding Energy

The signed interaction energy was calculated using the following equation:

$$E_{binding} = -E_{inter} = -(E_{total} - E_{component1} - E_{component2} - \ldots) \quad (1)$$

$$\Delta E = E(\text{PAA+ plasticizer}) - [E(\text{PAA}) + E(\text{plasticizer})]$$

$$E_{binding} = -\Delta E$$

A negative value of ΔE indicates that the combined system is energetically more stable than the isolated components. For clarity, the binding energy is expressed as the magnitude of the interaction energy and is defined as $E_{binding} = -\Delta E$. According, the positive values reported in Table 1 (40.02, 50.51, and 82.79 kcal mol^{-1} for PAA/BTTN, PAA/TMETN, and PAA/TEGDN, respectively) correspond to the magnitudes of the respective negative interaction energies.

On the magnitude basis used in the table 1, the largest value was obtained for TEGDN. These energy differences provide a comparative measure of interaction within the modeled bulk mixtures; they do not directly quantify plasticizer uptake, migration rate, interfacial retention, or adhesion.

Table 1. Binding energy in different systems in the presence and absence of plasticizer.

System	Total energy (kcal.mol^{-1})	Binding Energy (kcal.mol^{-1})
PAA	-839.05	-
BTTN	-1325.51	-
TMETN	-712.60	-
TEGDN	-131.42	-
PAA/BTTN	-2204.58	40.02
PAA/TMETN	-1602.16	50.51
PAA/TEGDN	-1053.26	82.79

The initial and final densities, along with their corresponding standard deviations, are summarized in Table 2. The relative standard deviations (RSDs), calculated as the ratio of the standard deviation to the corresponding final density, are approximately 2.33%, 1.84%, and 1.46% for PAA/BTTN, PAA/TMETN, and PAA/TEGDN, respectively. These values quantify the dispersion of the sampled final-density data and should not be interpreted as measures of the initial-to-final density deviation or, on their own, as evidence of complete configurational equilibration [17].

Table 2. Initial and final densities after500 ps.

System	Initial density (g cm^{-3})	Final density (g cm^{-3})	Standard deviation
PAA	1.200	1.229	0.023
BTTN	1.520	1.557	0.024
TMETN	1.470	1.495	0.023
TEGDN	1.330	1.338	0.020
PAA/BTTN	1.360	1.461	0.034
PAA/TMETN	1.338	1.415	0.026
PAA/TEGDN	1.269	1.369	0.020

3.2. Radial Distribution Function (RDF)

The radial distribution function (RDF) analysis was performed to investigate the overall radial distribution characteristics of the molecular systems. The RDF curves presented in Figure 10 were calculated based on the overall atomic configurations of each system, without selecting specific atom types or defining particular cross-component atom pairs. Therefore, these curves represent the total RDF behavior of the systems rather than specific correlations between PAA and the corresponding plasticizer. It should be noted that differences between the RDF profiles of the pure components and their mixtures may be influenced by changes in molecular packing and system composition, as well as by intermolecular interactions. Accordingly, the observed RDF differences should not be interpreted as direct or exclusive evidence of specific PAA–plasticizer interactions. Instead, the RDF results provide an overall description of the structural organization of the investigated systems and should be interpreted alongside the other calculated properties, including binding energy and solubility parameters.

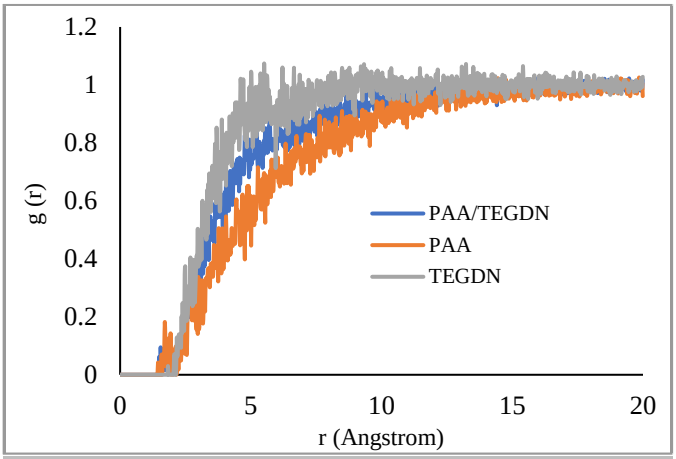


Fig 10. Total radial distribution function (RDF) obtained from the atomic configurations of the PAA–TEGDN system.

Figure 11 shows the RDF identified in the original analysis as intramolecular. Peaks at distances below 3 Å indicate short-range structural correlations, but their presence alone does not identify the physical origin of the peaks. Without a documented atom-pair selection and a separate energetic or angular analysis, these features should not be assigned specifically to electrostatic interactions; they may also reflect local molecular geometry and bonded or near-neighbor correlations [18, 19].

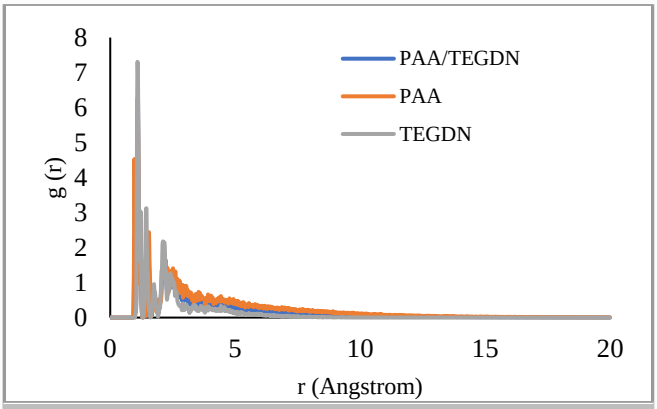


Fig 11. Intramolecular radial distribution function (RDF) obtained from the atomic configurations of the simulated system.

Figure 12 and Table 3 report free and occupied volumes at 0, 50, 100, 250, and 500 ps. According to the tabulated values, the minimum free volume occurs at 250 ps (1846.41 Å³), whereas the maximum occupied volume occurs at 100 ps (15705.86 Å³). The free volume at 500 ps is 1900.02 Å³; therefore, it is not the minimum among the reported snapshots. These values are discrete configurations rather than statistically converged time averages. They do not, on their own, establish that the system reached equilibrium after 100 ps or that the free volume decreased monotonically.

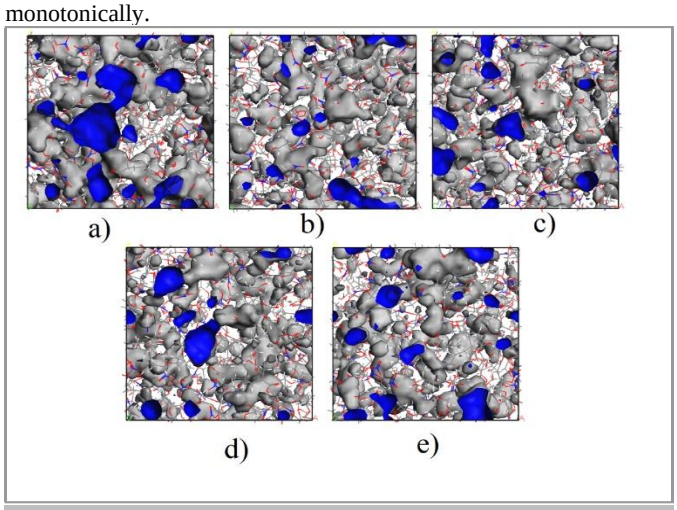


Fig 12. Free volume of polyacrylic acid and TEGDN at different times: (a) 0, (b) 50, (c) 100, (d) 250, and (e) 500 ps.

Table 3. Free volume and occupied volume of polyacrylic acid and TEGDN.

Time (ps)	Free volume (A^3)	Occupied volume (A^3)
0	3800.82	15070.21
50	2023.01	15581.31
100	2050.41	15705.86
250	1846.41	15687.33
500	1900.02	15596.39

3.3. Solubility Parameter

The solubility parameter is a useful empirical indicator for evaluating the potential compatibility between two components. A smaller difference between the solubility parameters generally indicates a closer match in their cohesive energy characteristics and, consequently, a higher potential for miscibility [15]. However, this parameter alone does not establish thermodynamic miscibility, since factors such as entropy of mixing, polymer chain length, composition, concentration, and specific polar interactions may also influence the miscibility of polymer–plasticizer systems. As shown in Table 4, the solubility-parameter differences between PAA and TEGDN, TMETN, and BTTN are 0.16, 0.93, and 2.85 $MPa^{1/2}$,

respectively. Accordingly, PAA/TEGDN exhibits the smallest difference and therefore the highest predicted compatibility among the investigated systems based on this criterion, followed by PAA/TMETN and PAA/BTTN [15, 20].

Table 4. Solubility parameters of polyacrylic acid and various plasticizers.

System	δ ($MPa^{1/2}$)
PAA	24.36
BTTN	27.21
TMETN	25.29
TEGDN	24.52

3.4. Mechanical Properties

The mechanical properties of the simulated systems were evaluated using the mechanical property calculation module in Materials Studio. The bulk modulus (K) and shear modulus (G) were directly obtained from the calculations using the Reuss averaging scheme, which is based on the uniform-stress assumption. Young's modulus (E) was subsequently derived from the bulk and shear moduli according to the following relationship [15]:

$$E = 9GK/(3K+G) \quad (2)$$

This relationship assumes isotropic linear-elastic behavior; therefore, the calculated Young's modulus values should be regarded as estimates based on an isotropic approximation of the elastic response of the simulated systems. As shown in Table 5, the Young's modulus decreased from 12.39 GPa for pure PAA to 11.62, 5.96, and 8.92 GPa for the PAA/BTTN, PAA/TMETN, and PAA/TEGDN systems, respectively. Among the investigated formulations, PAA/TMETN exhibited the greatest reduction in Young's modulus, followed by PAA/TEGDN and PAA/BTTN. These results indicate that plasticizer incorporation modifies the calculated elastic response of PAA, with the extent of this change depending on the type of plasticizer. The observed reduction in Young's modulus is consistent with a potential plasticization effect, although it does not, by itself, establish enhanced toughness, extensibility, or interfacial adhesion. Despite these reductions, the calculated Young's modulus values remain relatively high for an application requiring a compliant rubber interlayer. This observation should be interpreted in the context of the simplified molecular models employed in this study, which consist of finite, uncrosslinked PAA chains and do not explicitly account for the fully cured polymer network or the rubber–liner interface. Furthermore, the finite simulation-cell size and limited simulation timescale may affect the predicted mechanical response. In the absence of independent simulation replicas and a systematic uncertainty analysis, the reported values should therefore be interpreted primarily as comparative estimates for the modeled systems rather than definitive predictions of their macroscopic mechanical performance.

Table 5. Calculated elastic properties of PAA and the PAA–plasticizer systems. E denotes Young's modulus estimated from K and G using Equation 2; units: GPa.

System	K (GPa)	G (GPa)	E (GPa)
PAA	7.39	5.08	12.39
PAA/BTTN	7.74	4.65	11.62
PAA/TMETN	5.20	2.28	5.96
PAA/TEGDN	6.70	3.49	8.92

4.Conclusions

The prediction of the properties of chemical materials for various applications remains a significant challenge. One of the most effective approaches to addressing these challenges is molecular dynamics (MD) simulation. By simulating the chemical environment, molecular dynamics enables the investigation of material properties under different conditions. Polyacrylic acid (PAA), owing to its favorable intrinsic properties, can be used as a novel liner material. Therefore, studying and predicting the properties of its mixtures is of considerable value. As a unique liner, polyacrylic acid can prevent phase separation at the interfaces between different polymer layers by effectively absorbing energetic plasticizers with polar structures. Molecular dynamics simulations of polyacrylic acid in the presence of three polar plasticizers (TEGDN, BTTN, and TMETN) revealed its strong affinity for these additives, suggesting its potential to minimize plasticizer accumulation at the interfaces between different polymer layers. The strongest interaction was observed for the TEGDN plasticizer, with a binding energy of 82.79 $kcal.mol^{-1}$. Furthermore, the solubility parameters of the investigated plasticizers revealed that the difference between the solubility parameters of the plasticizers and polyacrylic acid was less than 3 $MPa^{1/2}$, indicating favorable miscibility. The calculated Young's modulus decreased from 12.39 GPa for pure PAA to 11.62, 5.96, and 8.92 GPa for PAA/BTTN, PAA/TMETN, and PAA/TEGDN, respectively. The lowest calculated Young's modulus was obtained for PAA/TMETN, followed by PAA/TEGDN. The RDF profiles describe structural correlations in the simulated systems; however, the available atom-pair information does not support assigning the short-range features specifically to electrostatic interactions or treating peak intensity as direct proof of miscibility. Taken together, the binding-energy magnitudes and solubility-parameter differences suggest favorable interactions and compatibility within the modeled PAA–plasticizer mixtures. These findings provide a preliminary molecular-level indication that PAA may be worth investigating as a plasticizer-absorbing liner. Its practical suitability, including absorption capacity, retention, mechanical compliance, and interfacial performance, requires further experimental and simulation-based validation.

Declaration of Competing Interest

The authors declare that they have no known competing financial interests or personal relationships that could have appeared to influence the work reported in this paper.

Acknowledgments

The authors are grateful to the Malek Ashtar University of Technology for supporting this work.

References

[1] T. Ünügül Yavuz, et al., Epoxidised natural rubber (ENR)/wollastonite composites for tyre Inner liners: A practical replacement for butyl rubber in industrial applications., Polym. Eng. Sci. 66.2 (2026) 1153-1169.
[2] A. L. Kwansa, R. C. Pani, J. A. DeLoach, A. Tieppo, E. J. Moskala, S. T. Perri, Y. G. Yingling, Molecular mechanism of plasticizer exudation from polyvinyl chloride. Macromol., 56(13) (2023) 4775-4786.
[3] Y. Guo, J. Liu, Y. Lu, D. Dong, W. Wang, L. Zhang, A combined molecular dynamics simulation and experimental method to study the compatibility between elastomers and resins. RSC adv., 8(26) (2018) 14401-14413.
[4] J.Y i, E. Keaney, J. Zhang, C. J. Hansen, W. Zukas, J. Mead, Improved adhesion in elastomeric laminates using elastomer blends. Rubber Chem. Technol., 95(3) (2022) 465-478.
[5] Y. Hao, F. Yang, Surface modification strategies for inhibiting the migration of plasticizers from plastics. Prog. Org. Coat., 210 (2026) 109697.
[6] W. Zhang, D. Niu, H. Xu, J. Xia, P. Xu, W. Yang, et al. Design of anti-migratory and thermally stable bio-plasticizers for polar plastics toward superior overall performance. J. Appl. Polym. Sci, 142(24) (2025) e57012.
[7] Z. Yu, W. Wang, W. Yao, W. Zhang, W. Xie, Y. Liu, et al., Simulation for the migration of nitrate ester plasticizers in different liners contacting with propellant by molecular dynamics. J. Energ. Mater., 39(1) (2021) 74-84.
[8] H. Li, W. Jiang, Y. Zhang, Z. Lu, Y. Hu, C. Xiao, et al., Solid propellant liner with high anti-migration and strong adhesion based on isocyanate-functionalized graphene oxide and hydroxy-terminated polybutadiene. J. Mater. Sci., 57(30) (2022) 14413-14429.
[9] L. Kong, K. Dong, Y. Tang, S. Lai, Molecular dynamics simulation of the influence of PEG-TDI aging degradation on diffusibility and compatibility of NG and BTTN. Propellants. Explos. Pyrotech., 46(9) (2021) 1436-1446.
[10] J. Gupta, C. Nunes, S. Vyas, S. Jonnalagadda, Prediction of solubility parameters and miscibility of pharmaceutical compounds by molecular dynamics simulations. J. Phys. Chem. B., 115(9) (2011) 2014-2023.
[11] H. L. Zheng, W. T. Wang, T. Liu, K. Ma, E. Zheng, W. W. Zhang, et al., Bio-based macromolecular polythiourethane plasticizers enable sustainable and migration-resistant flexible films for intelligent packaging. J. Mater. Chem. B., 14(13) (2026) 4048-4058.
[11] H. L. Zheng, W. T. Wang, T. Liu, K. Ma, E. Zheng, W. W. Zhang, et al., Bio-based macromolecular polythiourethane plasticizers enable sustainable and migration-resistant flexible films for intelligent packaging. J. Mater. Chem. B., 14(13) (2026) 4048-4058.
[12] S. S. Jagarlapudi, H. S. Cross, T. Das, W. A. Goddard III, Thermomechanical properties of nontoxic plasticizers for polyvinyl chloride predicted from molecular dynamics simulations. ACS Appl. Mater. Interfaces., 15(20) (2023) 24858.
[13] Q. Lei, X. Yi, W. Yu, J. Cheng, S. Ou, Q. Xue, H. Jiang, Molecular dynamics simulation of plasticizing effect of mixed dioctyl phthalate and isosorbide diheptanoate on polyvinyl chloride material., Polym., 17(12) (2025) 1655.
[14] I. Laib, D. E. Laib, S. Boucetta, C. Bengoechea, M. Felix, Molecular dynamics insights into essential oil-enriched biopolymer films: structural stability and functional performance for active packaging. Iran. Polym. J., (2026)1-30.
[15] F. Chen, H. Yang, Q. Lu, J. Yang, L. Xiao, Y. Wang, F. Zhao, W. Jiang, G. Hao Molecular dynamic simulation on the interaction and compatibility between ammonium dinitramide and typical fluoropolymers in solid propellants. Mater. Today. Commun. 35 (2023)106254.
[16] Y. Yang, Z. Liang, R. Zhang, S. Zhou, H. Yang, Y. Chen, et al. Research advances in superabsorbent polymers. Polym, 16(4) (2024) 501.
[17] G-y. Hang, W-l. Yu, T. Wang, J-t. Wang, Z. Li, Theoretical insights into effects of molar ratios on stabilities, mechanical properties and detonation performance of Cl-20/RDX cocrystal explosives by molecular dynamics simulation. J Mol Struct 1141 (2017) 577–583.
[18] T. Sun, J.J. Xiao, Q. Liu, F. Zhao, H.M. Xiao, Comparative study on structure, energetic and mechanical properties of a ε-Cl-20/HMX cocrystal and its composite with molecular dynamics simulation. J Mater Chem A 2(34) (2014)13898–13904.
[19] H. Abou-Rachid, L.S. Lussier, S. Ringuette, X. Lafleur-Lambert, M. Jaidann, J. Brisson, On the correlation between miscibility and solubility properties of energetic plasticizers/polymer blends: modeling and simulation studies. Propellants Explos Pyrotech 33(4) (2008)301–310.
[20] L. Sperling, J. Manson, Polymer blends and composites. Plennun, New York (1976).

How to cite this manuscript: Dariush Fallah*, Molecular Dynamics Simulation of Poly (acrylic acid) as a Liner at Rubber–Rubber Interfaces in the Presence of Nitrate Ester Plasticizers, Frontiers in Chemical Research, 2026, 3, 37-43, doi: 10.22034/fcr.2026.2108660.1034.